

Rapid postseismic transients in subduction zones from continuous GPS

Timothy I. Melbourne,¹ Frank H. Webb,² Joann M. Stock,³ and Christoph Reigber⁴

Received 7 May 2001; revised 5 January 2002; accepted 9 January 2002; published 22 October 2002.

[1] Continuous GPS time series from three of four recently measured, large subduction earthquakes document triggered rapid postseismic fault creep, representing an additional moment release upward of 25% over the weeks following their main shocks. Data from two $M_w = 8.0$ and $M_w = 8.4$ events constrain the postseismic centroids to lie down dip from the lower limit of coseismic faulting, and show that afterslip along the primary coseismic asperities is significantly less important than triggered deep creep. Time series for another $M_w = 7.7$ event show 30% postseismic energy release, but here we cannot differentiate between afterslip and triggered deeper creep. A fourth $M_w = 8.1$ event, which occurred in the broad Chilean seismogenic zone, shows no postseismic deformation, despite coseismic offsets in excess of 1 m. For the three events which are followed by postseismic deformation, stress transferred to the inferred centroids (at 34, 60, and 36 km depths) by their respective main shock asperities increased reverse shear stress by 0.5, 0.8, and 0.2 bar with a comparatively small decrease in normal stress (0.01 bar), constraining the Coulomb stress increase required to force slip along the metastable plate interface. Deep triggered slip of this nature is invisible without continuous geodesy but on the basis of these earthquakes would appear to constitute an important mode of strain release from beneath the seismogenic zones of convergent margins. These events, captured by some of the first permanent GPS networks, show that deep moment release is often modulated by seismogenic rupture updip and underscore the need for continuous geodesy to fully quantify the spectrum of moment release in great earthquakes. *INDEX TERMS*: 7209 Seismology: Earthquake dynamics and mechanics; 3040 Marine Geology and Geophysics: Plate tectonics (8150, 8155, 8157, 8158); 8150 Tectonophysics: Plate boundary—general (3040); 7230 Seismology: Seismicity and seismotectonics; *KEYWORDS*: subduction zone, earthquake, postseismic, moment release

Citation: Melbourne, T. I., F. H. Webb, J. M. Stock, and C. Reigber, Rapid postseismic transients in subduction zones from continuous GPS, *J. Geophys. Res.*, 107(B10), 2241, doi:10.1029/2001JB000555, 2002.

1. Introduction

[2] The characteristics of strain accumulation and release down dip of subduction zone seismogenic plate contacts are not well understood. Thermal and constitutive models of most subduction zones indicate that the plate interface transitions with increasing depth from purely stick-slip, seismogenic behavior to stable sliding, between which lies a regime where runaway fault rupture cannot self-nucleate. The frictional characteristics of this metastable region are complex. The interface here is thought to be able to both sustain seismogenic slip rates if triggered by dynamic

stresses accompanying incoming rupture fronts and also to be able to creep slowly, with rupture rates below that detectable by most forms of seismic instrumentation [Tse and Rice, 1986; Tichelaar and Ruff, 1993; Byrne et al., 1988; Hyndman and Wang, 1995; Marone and Scholz, 1988; Scholz, 1989; Dieterich, 1992]. Observationally, most laboratory constraints on the constitutive state here remain untested, primarily because of a lack of measured fault processes attributable unambiguously to the metastable region. Direct observation of strain accumulation uniquely along this portion of the plate contact has proven elusive because of the nonuniqueness of surface deformation inversions, as has, until recently, direct observation of slow moment release here. "Partial locking," or steady creep at a fraction of the convergence rate, has proven useful for modeling interseismic surface deformation to identify the locked region but makes little sense physically, given what is known about interplate contact friction. A velocity-weakening interface will not creep, yet a velocity-strengthening interface will accumulate shear stress across the interface until an equilibrium creep rate equal to the plate convergence rate is established. Neither state yields a long-term steady creep rate at a fraction of the convergence rate.

¹Department of Geological Sciences, Central Washington University, Ellensburg, Washington, USA.

²Jet Propulsion Laboratory, California Institute of Technology, Pasadena, California, USA.

³Seismological Laboratory, California Institute of Technology, Pasadena, California, USA.

⁴Kinematik und Dynamik der Erde, GeoForschungsZentrum Potsdam, Potsdam, Germany.

Since the metastable region is often inferred to be equal to or of greater total area than the seismogenic region, it represents a potentially important contribution to the energy budgets of subduction zones globally.

[3] Given the large increases in Coulomb stress generated along the tips of dislocations [Harris, 1998], it might be expected that great subduction earthquakes trigger, through shear loading of the down-dip metastable plate interface, quiet, postseismic fault creep here. This would introduce a time dependency of fault slip and healing, which, over the long term, could be mathematically described, on average, as partial locking if detailed temporal observations were absent. Add to this afterslip, or postseismic creep transients along main shock ruptures, predicted by rate- and state-dependent friction and observed in both continental transform settings and subduction zones [Marone et al., 1991; Scholz, 1998; Lapusta et al., 2000; Smith and Wyss, 1968; Bucknam et al., 1978; Prescott et al., 1984; Shen et al., 1994; Nakano and Hirahara, 1997; Bürgmann et al., 1997; Ueda et al., 2001; Heki et al., 1997; Bürgmann et al., 2001], and the paradigm of simple stick-slip behavior begins to appear misleadingly simple.

[4] Estimates of moment release based solely on radiated seismic energy along subduction zones generally fall below that expected from plate convergence rates alone [Kanamori, 1977; Kanamori and Astiz, 1985], which may in part reflect aseismic moment release. Long-term postseismic transients acting over years to decades have long been recognized from campaign mode occupation of leveling and triangulation networks, but to fully understand the energy budget associated with convergent margins requires filling in the spectral holes that lie between seismogenic fault processes and year timescale strain release. Historically, any rapid postseismic deformation following in the hours, days, weeks, or months after past earthquakes would have been wrongly attributed to coseismic moment release upon subsequent campaign remeasurement [Prescott and Lisowski, 1977; Thatcher and Fujita, 1984; Thatcher, 1984; Linde and Silver, 1989; Savage and Plafker, 1991; Barrientos et al., 1992; Cohen, 1998]. Indeed, the recent deployment of continuous GPS receivers along side campaign measurements at convergent margins now suggests that the dearth of reported transients may, in fact, be due as much to a lack of continuous observations as to a lack of genuine transients [Heki and Tamura, 1997; Lowry et al., 2001].

[5] Here we present time series from four large subduction earthquakes, three of which, the 1995 $M_w = 8.0$ Jalisco, Mexico, the 2001 $M_w = 8.4$ Peru, and the 1994 $M_w = 7.7$ Sanriku-Oki, Japan earthquakes, show significant aseismic moment release which we estimate to amount to nearly 35%, 20%, and 30% of main shock moment release over the weeks following the event (Figure 1). A fourth event, the $M_w = 8.0$ 1995 Antofagasta, Chile, event, showed no such deformation within a few parts in a thousand, despite coseismic offsets in excess of 1 m. This fourth event is unique among the set of four in that it occurred directly updip of two $M_w = 7.5$ (1987) and $M_w = 7.2$ (1988) events within the exceedingly broad seismogenic portion of the Chilean subduction zone and was followed in 1998 by a $M_w = 7.0$ event also directly down dip of primary rupture region, discussed further below. In the three regions which do show postseismic deformation, the rapid evolution of the

signal and our existing knowledge of crustal and mantle wedge viscosities [Winder and Peacock, 2001; James et al., 2000] require that the observed deformation be attributed to slow faulting along the plate interface rather than crustal or mantle relaxation processes.

1.1. Data Analysis

[6] Deformation accompanying all earthquakes was measured with dual-frequency P code receivers and processed using the GIPSY-OASIS II software [Lichten and Border, 1987] and ephemerides and satellite clock corrections provided by the International Geodynamics Service [Zumberge et al., 1995]. In this process, station coordinates, carrier phase biases, zenith troposphere delays, and station clocks were estimated using 24-hour data arcs. Station coordinates were processed using 2-hour (Japan and Peru), 6-hour (Mexico), and daily (Chile) stochastic coordinate resets, depending on the signal-to-noise ratio at the higher estimation rates and the deformation power contained in the higher frequencies. By applying stochastic resets to the coordinates only, the geometric strength of the 24-hour data arc for estimating the carrier phase biases and atmospheric delays is retained, and station position estimates are obtained at a higher rate without significant systematic error associated with the higher-frequency error sources. Phase biases were estimated as real valued parameters and the double-differenced biases were fixed to their dual-frequency integer equivalents using the method of Blewitt et al. [1993]. In all cases, >90% of the double-differenced phase biases were resolved.

1.1.1. The 1995 Jalisco, México ($M_w = 8.0$), Event

[7] The Jalisco, México, GPS network lies primarily within the states of Jalisco, Colima, and Michoacan and was installed 18 months prior to the $M_w = 8.0$ earthquake of 9 October 1995 to study the influence of the subduction of the Rivera plate on the tectonic evolution of continental North America [DeMets et al., 1995]. It was first occupied 6 months prior to the event and reoccupied 6 days afterward. Inversion of the GPS measurements revealed shallow coseismic faulting concentrated in two asperities located largely above 18 km depth, one of which reached 5 m of displacement, which together produced regional subsidence and extension throughout the network [Melbourne et al., 1997]. In the context of constraining the down-dip limit of coseismic faulting, there is good agreement between the local GPS inversion and that derived from the teleseismic analyses. This proves important for differentiating between postseismic afterslip along the main shock asperities and postseismic slip triggered distal, in this case, down dip, to the main shock rupture. Three different methods of teleseismic analysis consistently show two primary asperities at depths above 15 km, shallower than the geodetic inversion (above 18 km) but at similar distances along strike from the centroid moment tensor (CMT) centroid [Dziewonski et al., 1997; Mendoza and Hartzell, 1999; Escobedo et al., 1998; Courboux et al., 1997]. The seismological estimates of the shallower slip distribution are probably the better estimate, given that the GPS inversion is hindered by having only mainland coastal stations and therefore becomes increasingly insensitive to variations in progressively shallower faulting. GPS stations on offshore islands, of which there are none here, could

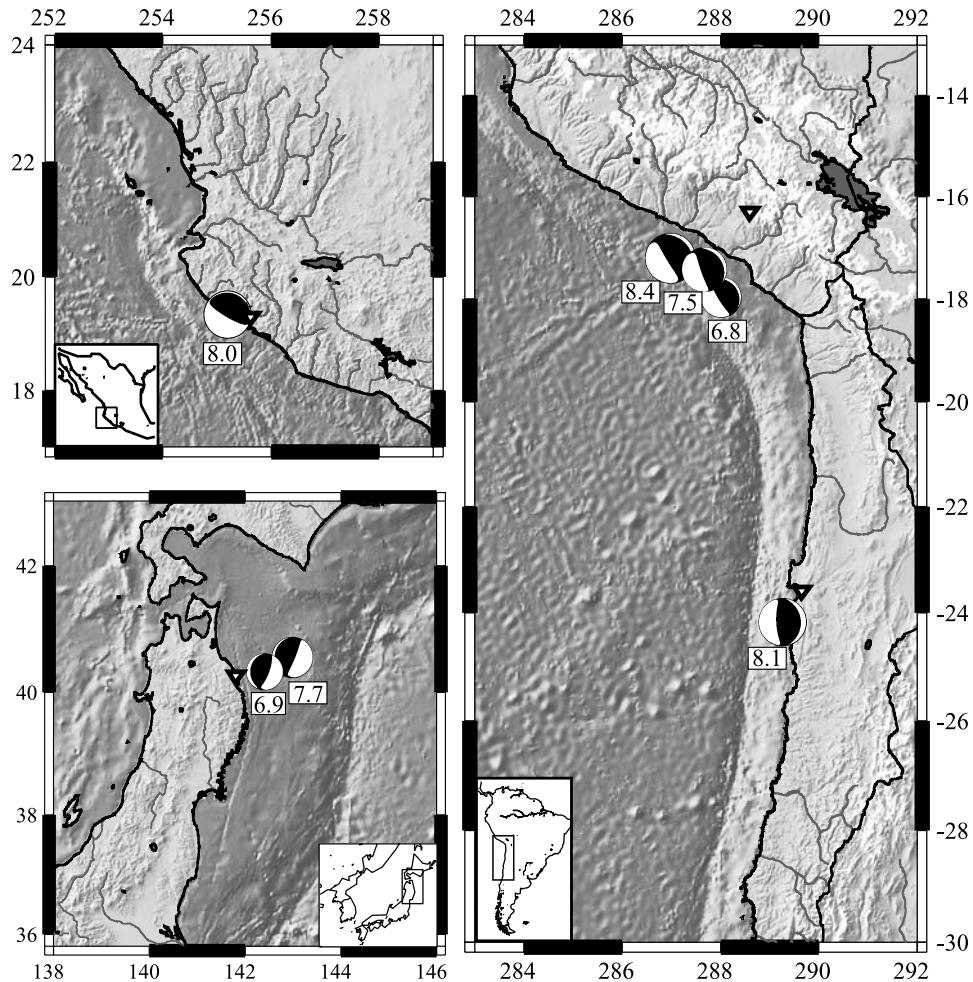


Figure 1. Locations of great subduction zone earthquakes monitored by continuous GPS discussed here. (top left) The 1995 Jalisco-Colima $M_w = 8.0$ event ruptured the interface between the subducting Rivera plate and North America. (bottom left) The 1994 $M_w = 7.7$ Sanriku-Oki event broke the Pacific-Asia plate boundary. (right) The 2001 $M_w = 8.4$ Peru earthquake ruptured the Nazca–South American plate interface and was followed by several large aftershocks visible on the GPS times. The 1995 $M_w = 8.1$ Antofagasta, Chile, earthquake also ruptured the Nazca–South American plate boundary. For all plots, open inverted triangles denote the location of the continuous GPS receivers, Harvard CMT focal mechanisms [Dziewonski *et al.*, 1997] are shown, and moment magnitudes (M_w) are labeled.

help differentiate the extent of shallow slip. Also, the homogeneous elastic half-space analytical functions embedded in the GPS inversion do not take into account radial variations in rigidity, which can be extreme over the hanging wall of a subduction zone and can introduce systematic biases [Masterlark *et al.*, 2001; James *et al.*, 2000; Okada, 1993]. Nonetheless, as our inferred location of faulting that produced the rapid postseismic deformation lies nearly 60 km down dip of the inferred lower limits of faulting from both GPS and teleseismic analyses, these differences are nonconsequential.

[8] One coastal station at Manzanillo Bay, continuously occupied for 9 days in March 1995, was reoccupied continuously for 9 days starting day 6 following the earthquake (Figure 2). Three tide gauges, one colocated with the GPS receiver in Manzanillo Bay and two far-field stations at Puerto Vallarta and Acapulco, ran continuously during the earthquake. Filtered and differenced daily tidal levels provided by Universidad Nacional Autónoma de México aver-

aged from 6-min measurements are used to estimate vertical deformation during the 6 days not measured with GPS. Since these are daily averages, and the Jalisco earthquake occurred midday, the coseismic subsidence appears across the day break. Together, both the filtered and differenced tide data indicate 14 ± 2 cm of coseismic subsidence, followed by 7 ± 2 cm of uplift between the main shock and the start of the GPS reoccupation on day 6 (Figure 2) [Ortiz *et al.*, 2000]. GPS reoccupation at day 6 showed 8.0 ± 1.3 cm of subsidence at Manzanillo, in agreement with tidal estimates assuming negligible strain accumulation during the 6 months prior to the main shock. Horizontal motion during this time measured 50 ± 0.8 cm southwest at azimuth 213° . Continuous GPS solutions from postearthquake day 6 to day 15 indicate an additional 4.5 ± 1.0 cm vertical uplift and continued 4.2 ± 1.0 cm of southwest extension at nearly the same azimuth 218° , indicating a slowing of postseismic deformation with time. There were no significant aftershocks with $M_w \geq 5.6$ during this time [Dziewonski *et al.*, 1997].

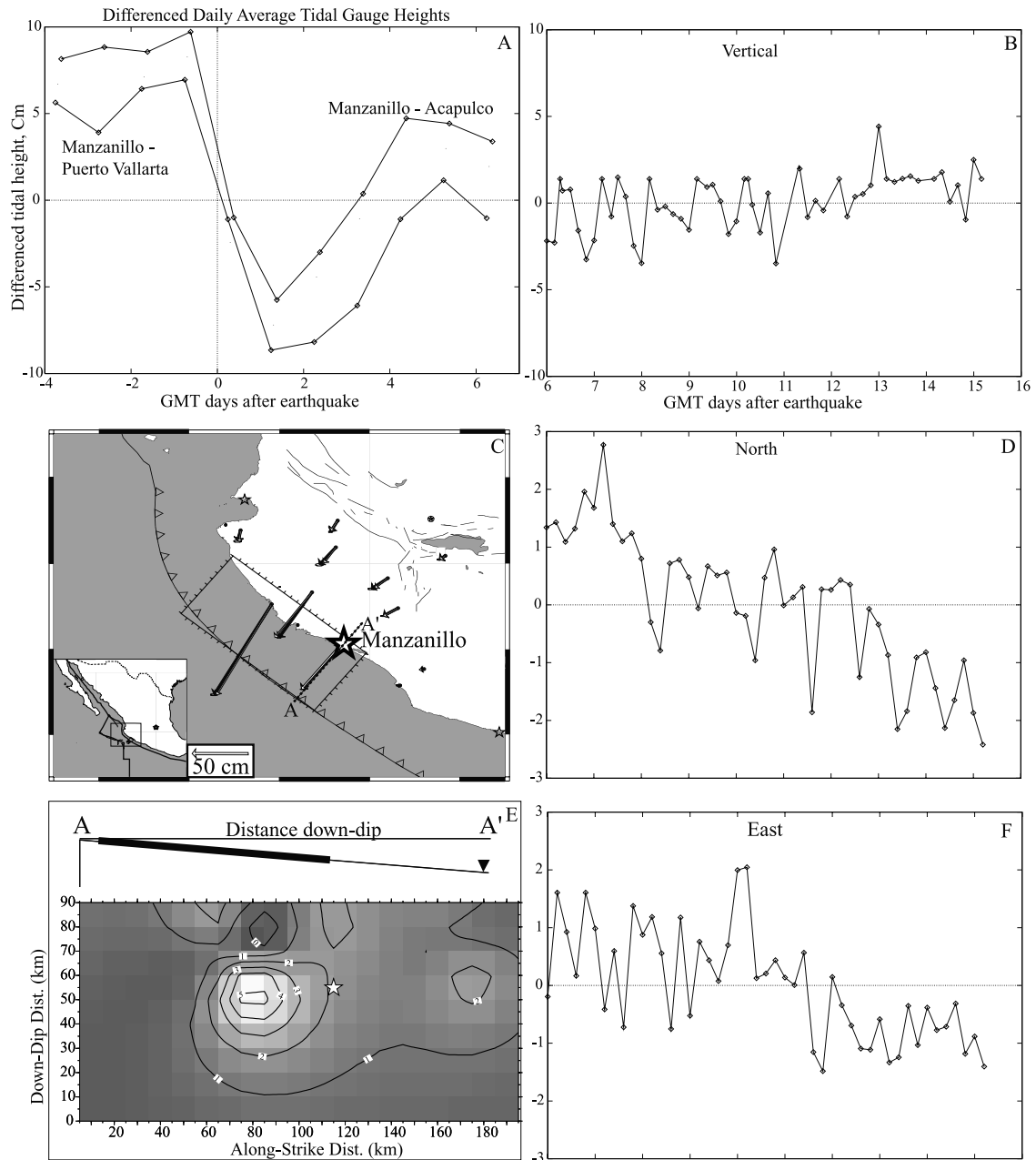


Figure 2. Ultrarapid postseismic deformation following the $M_w = 8.0$ 1995 Jalisco earthquake recorded by GPS and tide gauge measurements. (a and c) Differenced and filtered tidal measurements indicate that coseismic subsidence of 14 cm at MANZ was followed by 7 ± 2 cm uplift over 6 days. (b) The 6-hour GPS solutions show continued uplift of 4.5 ± 1.0 cm between day 6 and day 15. (d and f) Horizontal motion during this time at MANZ is continued southwest extension similar to the coseismic motion. (c) Solid arrows are data. (e) Open arrows are forward calculations based on the coseismic variable-slip distribution from *Melbourne et al.* [1997]. Profile along line A-A' in Figure 2c is shown in Figure 2e; heavy solid line indicates depth extent of coseismic faulting, and triangle shows inferred depth of postseismic centroid. Tide gauges (small stars) include one collocated with the GPS station in Manzanillo (Figure 2c) and two located in the far field at Puerto Vallarta and Acapulco. Standard deviations in north, east and up components, not plotted for clarity, measure 0.4, 0.6, and 0.9 cm, respectively.

[9] Since the continuous data are limited to one station, it is not possible to perform a network inversion to image the postseismic slip distribution, as was done for the coseismic and multiyear postseismic deformation. Nonetheless, the available three-component deformation vector offers simple

geometric constraints about the average amount and location of the postseismic slip which immediately followed the main shock. These inferences, although based on temporally limited data, are borne out by subsequent campaign reoccupation of the Jalisco network over the following 5 years,

discussed further below. In particular, the vertical motion is very diagnostic of the depth extent of faulting along the plate interface. Coseismic subsidence followed by rapid postseismic uplift without change in horizontal azimuth requires reverse faulting down dip of the main shock rupture, beneath the GPS station rather than offshore from it. Significant afterslip along the coseismic rupture plane, such as that predicted by rate- and state-dependent constitutive relations alone [Scholz, 1998] would produce additional postseismic subsidence rather than the observed uplift, while slip propagation along strike would vary the horizontal azimuths. While the resolution limitations of the coseismic slip distribution inverted from the full 15-station GPS network offsets have been discussed previously [Melbourne *et al.*, 1997], it is important to note that between the GPS and teleseismic analyses the lower limit of seismogenic faulting is particularly well determined for this event, probably to within ± 5 km along the plate interface. Thus there is no feasible way to produce postseismic uplift at Manzanillo except through faulting down dip of the coseismic rupture plane. A significant along-strike migration of slow slip from the coseismic asperity, in turn, would alter the azimuth of horizontal postseismic deformation, which for these data matches the coseismic. Thus the three-dimensional GPS offsets at Manzanillo derived from the vectors measured over 9 days following the event yield a best fitting postseismic slip centroid (a point source dislocation) located at 35 km depth, or 60 km down dip from the lower limit of coseismic slip. This lies within a region which did not rupture during the main shock. This centroid, of course, represents only the average postseismic slip location, and is geometrically constrained by the fact that slip significantly shallower or deeper than the centroid would produce subsidence rather than uplift and misfit in horizontal to vertical deformation ratios, respectively.

[10] Our inference from the postearthquake data of rapid, deep creep occurring well below the coseismic asperities is confirmed by subsequent campaign reoccupation of the full 26-site Jalisco GPS network in early 1996, 1997, and 1998. Hutton *et al.* [2002] find the network to be characterized by continued vertical uplift and southwest extension of up to several centimeters between postearthquake October 1995 and March 1999. From this they conclude that upward of 0.4 m of slip occurred at down-dip distances of up to 110 km before March 1996, or 50 km down dip from the primary coseismic asperity imaged by Melbourne *et al.* [1997]. From 1996 to 1999 they image continued slip of up to 20 cm down dip of the coseismic asperity and negligible slip along the coseismic asperity itself. Thus the deep creep which we image appears to have begun with the main shock and slowly decayed over the following years.

[11] It is possible to estimate the postseismic moment budget by making some assumptions about the postseismic fault plane. If we treat the 14 cm of coseismic subsidence and 11 cm of postseismic uplift which occurred during the weeks following the Jalisco event as a proxy for the total strain release but account for the difference in centroid-receiver distances, the postseismic offset indicates an additional aseismic moment release of 35% of the main shock, or the equivalent of an $M_w = 7.7$ event. This is less than than the 70% estimated by Hutton *et al.* [2002] by integrating inferred postseismic creep recorded after main shock

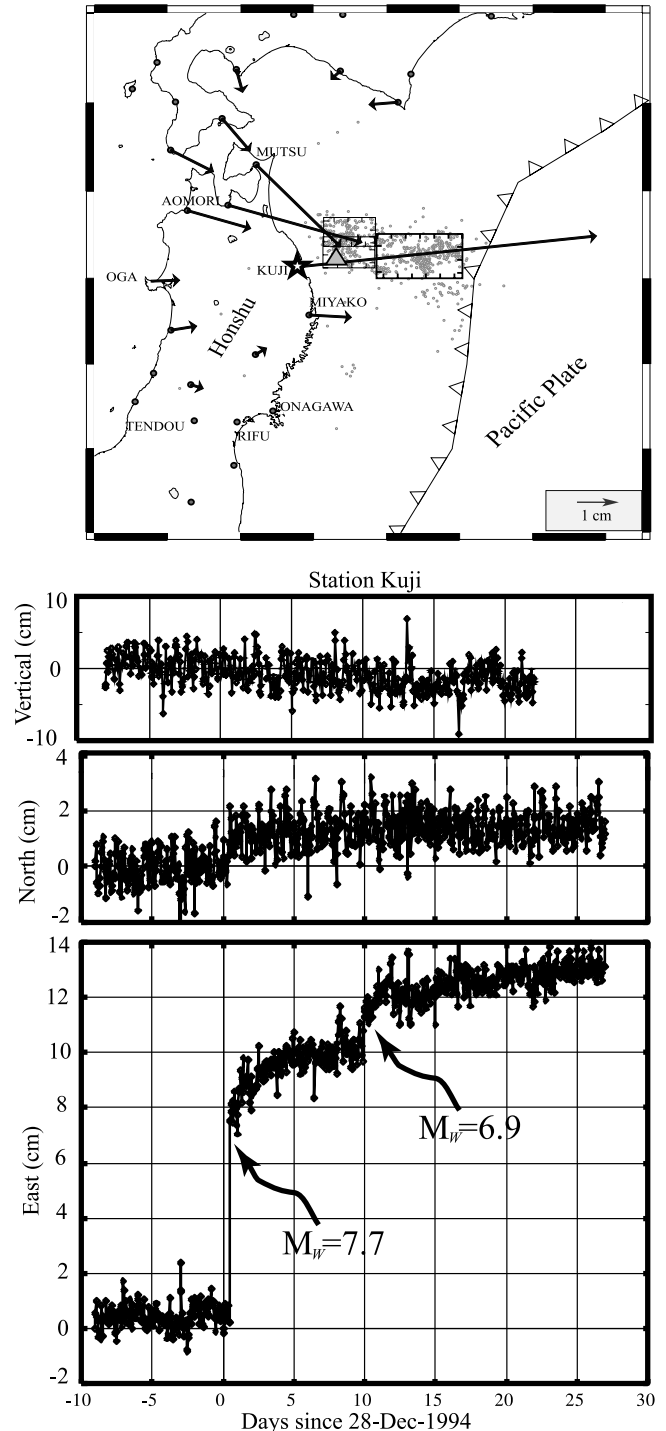
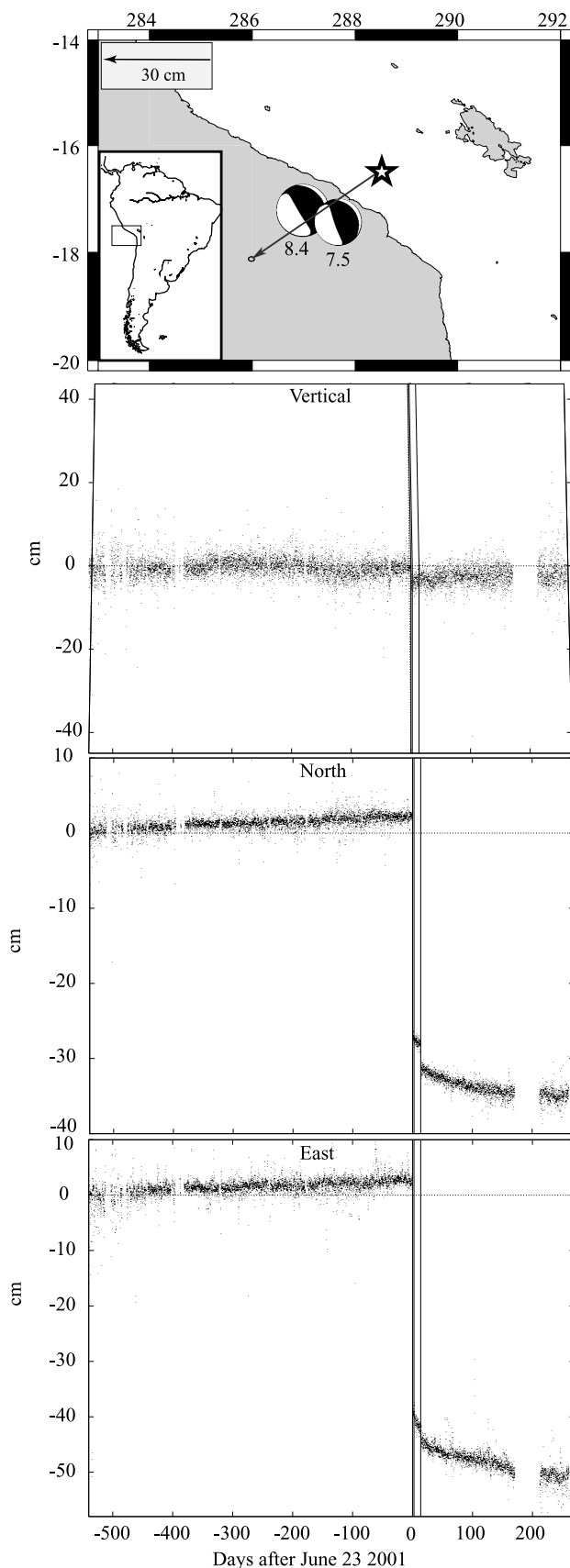


Figure 3. Ultrarapid postseismic deformation following the $M_w = 7.7$ 1994 Sanriku-Oki event. Approximately 7.75 ± 1.0 cm of easterly offset is followed by an additional 2.25 ± 1.0 cm over 10 days. The $M_w = 6.9$ aftershock appears to demonstrate a similar phenomenon near the detection level. Vertical uplift accompanying the event is consistent with faulting occurring nearly beneath station KUIJI. Slip distribution is adapted from Heki *et al.* [1997]. Formal errors in north, east, and up components measure 0.4, 0.7, and 1.3 cm, respectively.



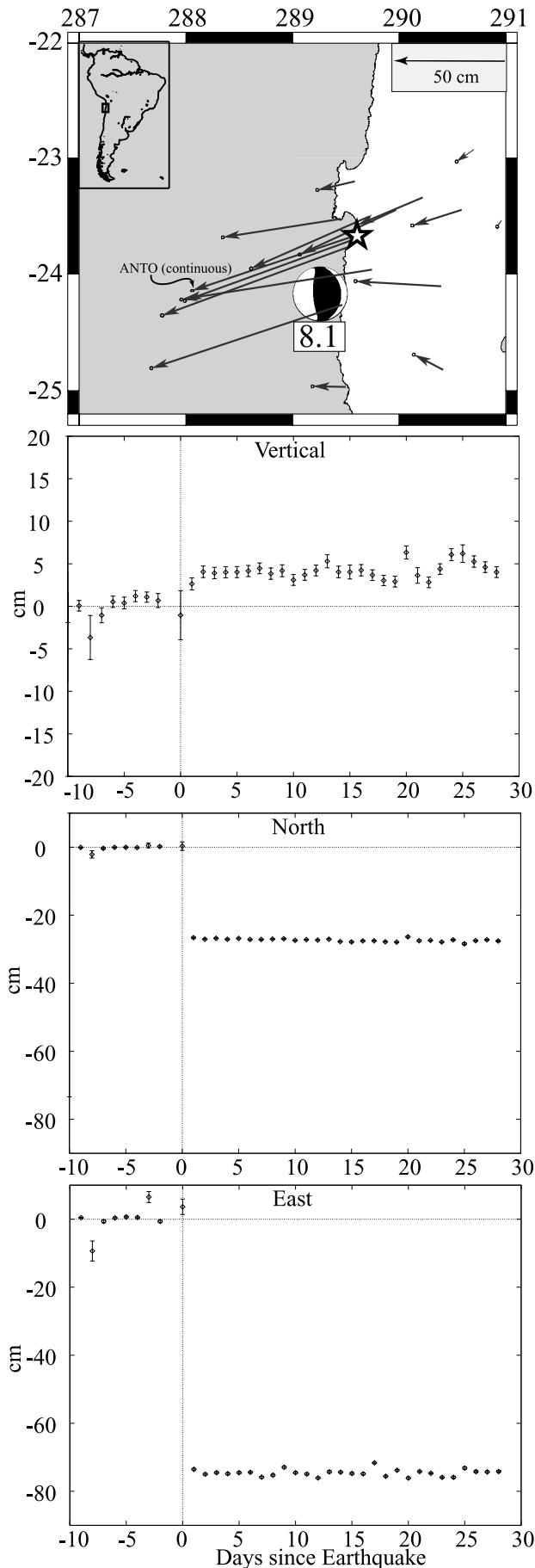
through 1999 but only includes the 2 weeks following the event, during which time postseismic deformation rates are highest [Heki and Tamura, 1997; Bucknam *et al.*, 1978; Scholz, 1998].

[12] From these measurements we can also estimate creep and moment release rates. The data cannot resolve between a propagating creep front analogous to a slow version of the Heaton pulse mechanism for fault failure [Heaton, 1991] versus far-field creep triggered by static stress increases from the main shock rupture. For the former mechanism the average slip front migration velocity between the main coseismic asperity and the inferred postseismic centroid is 5 cm/s over the 15-day observation window. However, the creep appears to have started immediately after the main shock (Figure 2a), and continued throughout the continuous GPS observation period, decaying over several years. Thus it seems likely that the latter mechanism, a uniform creep relaxation along the deeper plate interface, accommodated the static stress increases produced by the main shock rupture updip.

[13] We can estimate the stress changes required to trigger and initiate such slip beneath Jalisco. Finite dislocations all produce large Coulomb stress increases in the vicinity of their edges, which in this case can be calculated using the coseismic slip distribution inverted from the full GPS network. For all four of the earthquakes described in this paper, Coulomb stress changes due to main shock slip estimations are calculated following Harris [1998] and Stein *et al.* [1994]. The Jalisco main shock increased reverse shear stress across the plate interface at the inferred postseismic centroid by 0.2 bar and decreased normal stress by 0.01 bar, resulting in a large positive increase in Coulomb stress for all positive values of an effective coefficient of friction [Harris, 1998]. If normal stress decrease is negligible compared to ambient normal stress, then the aseismic, conditionally stable plate interface here is held within 0.2 bar of shear failure between repeating shallow seismogenic events. Note that this is only an estimate of the stress increase required to start and sustain deep slip. The absolute in situ stress magnitudes are not known, and these data do not relate to them.

[14] By making some additional assumptions about the spatial extent of the afterslip we can estimate the order of magnitude of slip at depth. If creep occurred along a down-dip extension with an along-strike width comparable to the primary main shock asperity and down-dip length compa-

Figure 4. (opposite) Two-year time series from Arequipa, Peru, clearly showing coseismic and postseismic offsets from the 2001 $M_w = 8.4$ earthquake sequence. Vertical bars indicate time of major aftershocks reported by in the Harvard CMT catalog. At the time of writing (October 2001), postseismic deformation at the Arequipa receiver continues to dominate the interseismic strain accumulation, although the rate is steadily declining, similar to comparable decay seen elsewhere. Coseismic subsidence followed by postseismic vertical uplift is explained by postseismic creep down dip of the main shock, beneath the station rather than offshore of it. Formal errors for the 2-hour position estimates for the north, east, and up components are 0.7, 0.9, and 1.8 cm, respectively.



erable to the coseismic and postseismic centroid spatial separation, similar to what is observed from campaign reoccupation of the Jalisco network over subsequent years, then 250 cm of cumulative slip over 15 days following the main shock is required to fit the postseismic time series, compared to the >500 cm of main shock slip. This represents an average slip rate of 16 cm/dy, which, of course, scales inversely with the assumed slip area.

1.1.2. The 1994 Sanriku, Japan ($M_w = 7.7$), Event

[15] Two-hour solutions from the Japanese National Network (JNN) GPS station Kuji nearest the 1994 Sanriku-Oki epicenter show a similar postseismic behavior, with coseismic easterly offsets of 7.75 ± 1.0 cm followed by an additional 2.25 ± 1.0 cm over 10 days (Figures 1 and 3). This indicates a 30% additional moment release if postseismic slip is located along the coseismic faulting plane, as was inferred for slip over year-long timescales [Heki *et al.*, 1997; Heki and Tamura, 1997]. The geometry of the JNN stations is insensitive to the down-dip extent of faulting due to the lateral distance between the nearest coastal station KUIJI and the coseismic rupture offshore. Thus it is not possible here to differentiate between afterslip purely along the coseismic rupture and deeper creep. Available coseismic slip inversions derived from teleseismic and regional seismic recordings predict that regional reverse shear stress increased along the inferred year-long postseismic fault on the order of 0.5 bar, twice that observed at Jalisco [Tanioka *et al.*, 1996; Heki *et al.*, 1997; Nishimura *et al.*, 1996]. The normal stress again drops by an amount smaller than a factor of 50 of the shear stress increase, again leading to large Coulomb stress increases. Regardless of whether the coseismic and postseismic slip is collocated, the creep would suggest that the plate boundary here is not strongly coupled, as has been suggested elsewhere [Pacheco *et al.*, 1993]. Discounting normal stress change indicates that the conditionally stable aseismic contact here lies within 0.5 bar of failure between events.

1.1.3. The 2001 Peru ($M_w = 8.4$) Event

[16] The 23 June 2001 $M_w = 8.4$ earthquake released the largest moment of any event in the last 30 years and produced over 50 cm of coseismic offset at the permanent GPS tracking station at Arequipa, Peru (AREQ), located roughly 100 km from the coast (Figure 1). AREQ forms part of the International GPS Service global tracking network used to estimate GPS satellite orbits [Zumberge *et al.*, 1995]. Preliminary source inversions for the main shock place between 1 and 8 m of thrust slip over a broad $200 \text{ km} \times 300 \text{ km}$ asperity centered to the southwest of Arequipa (M. Kikuchi and Y. Yamanaka, Earthquake Information Center seismological note 105, Earthquake Information Center, Earthquake Research Institute, University of Tokyo, 2001, available at http://www.eri.u-tokyo.ac.jp/EIC/EIC_News/105E.html; hereinafter referred to as Kikuchi and Yamanaka, electronic publication, 2001). From the main shock until the

Figure 5. (opposite) Continuous time series from the $M_w = 8.0$ 1995 Antofagasta, Chile, earthquake show no postseismic deformation, despite coseismic offsets in excess of 1 m. The down-dip extension of the 1995 rupture broke in 1987, which likely inhibited induced creep following this event. Errors plotted are 2σ .

time of this writing, 5.0 ± 1.3 cm of coseismic subsidence and 50 ± 10.8 cm of southwest extension have been followed over the past 4 months by 4 ± 1.3 cm of decaying vertical uplift and 9.5 ± 1.0 cm of continued southwest directed extension. Here we have corrected for interseismic strain accumulation at rates estimated from the 2 years of data prior to the earthquake. As of early 2002 the station continues to move, although the rate of postseismic deformation is steadily declining (Figure 4). As with the Jalisco earthquake, the postseismic rebound is diagnostic of creep down dip of the main shock, under the AREQ GPS station rather than offshore of it. The best fitting postseismic centroid lies beneath and slightly southwest of AREQ, along the same azimuth as the 8-m slip patch imaged by Kikuchi and Yamanaka, (electronic publication, 2001) but at the lower limit of their inferred 1-m slip contour. Interpreting the postseismic deformation as a proxy for postseismic moment release and accounting for the difference between the postseismic centroid-AREQ distance and the coseismic centroid-AREQ distance yields roughly a 20% additional moment release during the 4 months since the event. The Kikuchi and Yamanaka (electronic publication, 2001) slip distribution can also be used to estimate Coulomb stress changes at the postseismic centroid which, like the Jalisco and Sanriku events, produces both large increases in reverse shear stress of 0.8 bar along with decreases in fault-normal stress, again resulting in large positive Coulomb stresses for all reasonable coefficients of fault friction.

1.1.4. The 1995 Antofagasta, Chile ($M_w = 8.1$), Event

[17] By way of contrast, the 1995 Antofagasta, Chile, earthquake, recorded on the GeoForschungsZentrum Potsdam SAGA network, showed no such deformation following the event, despite coseismic offsets in excess of 1 m [Klotz *et al.*, 1999], nicely illustrating a global heterogeneity in interplate coupling styles (Figure 5). Although well-located aftershocks show clustering extending to depths of 50 km along the plate interface [Sobiesiak, 2000; Husen *et al.*, 1999], available estimates from the SAGA GPS array, teleseismic inversions, and InSAR all confine the 1995 slip to shallower than 35 km, or roughly only the upper half the seismogenic zone as estimated from thermal models of the plate interface [Delouis *et al.*, 1997; Ihmlé and Ruegg, 1997; Klotz *et al.*, 1999; Carlo *et al.*, 1999; Pritchard *et al.*, 2002; Comte *et al.*, 1994; Comte and Suarez, 1995; Aruajo and Suarez, 1994; Oleskevich *et al.*, 1999]. This may be a key difference in terms of explaining the lack of any observable postseismic creep. The 1995 event was both preceded and succeeded by $M_w = 7$ earthquakes down dip of the 1995 rupture. A $M_w = 7.5$ event broke below the center of the 1995 slip, followed by a $M_w = 7.2$ down dip event of the southern region in 1988. In 1998 an $M_w = 7.0$ event occurred down dip of the northern half of the 1995 event [Dziewonski *et al.*, 1997; Carlo *et al.*, 1999], which is probably related to the Antofagasta main shock.

[18] The slip distributions for the Antofagasta event predict reverse shear stress increases at the metastable transition to be less than that observed at Jalisco and Sanriku, but not substantially so. The 0.1 bar of shear stress increase and 0.01 bar decreased normal stress primarily reflect the greater distances involved in the Chilean convergent margin to the inferred metastable region. Thus it is not clear why the Chile event was not succeeded by any

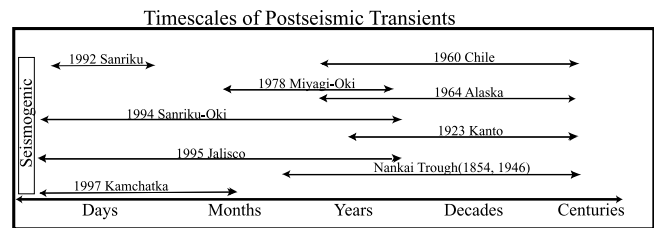


Figure 6. Observed spectrum of postseismic moment release following great subduction earthquakes. Older events, measured with campaign triangulation or leveling, show deformation over months to years. More recent events, captured with continuous GPS, indicate that rapid steady decay of deformation occurring over timescales starting at the seismogenic and extending through hours, days, and weeks is not unusual. The division between these two categories is thus governed more by the nature of the observations than the nature of the postseismic deformation. Together, these reports would suggest that great subduction zones do not stop abruptly but steadily decay into slow slip down dip of their seismogenic zones, thus deforming postseismically over all timescales, with spectral power, not necessarily equal, ranging from seconds to centuries. References are for 1960 Chile, *Linde and Silver* [1989] and *Barrientos et al.* [1992]; 1992 Sanriku, *Kawasaki et al.* [1995]; 1994 Sanriku, *Heki et al.* [1997] and this study; 1995 Jalisco, *Melbourne et al.* [1997], *Ortiz et al.* [2000], *Hutton et al.* [2002], and this study; 1964 Alaska, *Prescott and Lisowski* [1977], *Cohen* [1998], and *Savage and Plafker* [1991]; 1923 Kanto, *Thatcher and Fujita* [1984]; Nankai Trough, *Thatcher* [1984]; 1995 Antofagasta, *Klotz et al.* [1996]; 1997 Kamchatka, *Kogan et al.* [1999] and *Bürgmann et al.* [2001]; 1978 Miyagi-Oki, *Ueda et al.* [2001].

detectable moment release. Dislocation modeling indicates that slip of more than a few decimeters at the transition would be observable at the continuous GPS station.

[19] Even more enigmatic is the dearth of afterslip along the main shock fault, which is resolvable to within a few parts in a thousand of the main shock with current GPS accuracy. This fact raises the question of whether most formulations of state-dependent friction laws, which imply a healing distance over which postseismic afterslip should occur, are applicable to this interface [Scholz, 1998]. There is some hint of postseismic deformation, currently under study with InSar [Reigber *et al.*, 1997], which has occurred over the years since the event. However, this deformation is not regionally consistent with elastic strain release along the plate interface and, due to the longer timescales over which it seems to be occurring, is more difficult to directly relate to interface creep.

2. Discussion

[20] The earthquakes described here are some of the first to be continuously monitored with GPS. That three out of four of them show continuous and rapid aseismic strain release would indicate that these large events typically decay into seismically undetectable slow slip rather than ending abruptly. Two of them clearly show that slip along

the deeper metastable region can be modulated by rupture updip. This has implications for both moment tabulation as well as earthquake nucleation and the concept of characteristic earthquakes in subduction zones.

[21] First, it is important to note that only the recent installation of continuous geodetic monitoring has permitted observation of this phenomenon. Comparable slow moment release in historical earthquakes, observed without continuous measurements, would be erroneously attributed to coseismic release if campaign-style reoccupation took place even weeks or months following the main shock. For vertical leveling, a traditional method, this can significantly skew the estimated amount of slip, since the postseismic vertical deformation often shows opposite polarity of the coseismic. This is illustrated by Figure 6, which presents well-studied earthquakes in which postseismic deformation has been documented. The events fall into two natural categories whose division appears governed more by the nature of the observations than the nature of the postseismic deformation. The first group consists of the recent events which were continuously monitored and show postseismic deformation detectable over timescales of days to years. For these events, insufficient time has passed to judge whether the observed deformation will continue over decades or longer. The second group consists of older events whose postseismic deformation has been intermittently recorded with leveling and triangulation. These events all show deformation that continues today, but the intermittency of the observations does not resolve shorter timescale deformation. Together, these reports suggest that most subduction zones deform postseismically over all timescales, with spectral power, not necessarily equal, ranging from hours to centuries.

[22] Just as main shocks load the deeper plate contact, postseismic slip here will tend to reload the seismogenic zone updip. Such reciprocal stress transfer could lead to complex recurrence intervals and suggests that the concept of characteristic earthquakes may not be readily applicable to subduction zones. Moreover, continuous GPS has established a wide variety of moment release styles, all of which are invisible to seismology and campaign geodesy, which will impact recurrence intervals. These include both silent earthquakes, deformation events lasting days, weeks, and months without the presence of an earthquake [Kawasaki et al., 1995; Dragert et al., 2001; Lowry et al., 2001; Freymueller et al., 2001] and short-term postseismic transients decaying over years and months [Nakano and Hirahara, 1997; Heki et al., 1997; Heki and Tamura, 1997; Kogan et al., 1999; Bürgmann et al., 2001]. Continuous GPS measurements have also indicated overall variability in interplate coupling, documenting freely slipping convergent margins showing negligible strain or seismicity [Savage and Lisowski, 1986; Freymueller and Beavan, 1999], strongly coupled seismogenic interfaces [Mazzotti et al., 2000], along-strike variation between slight and full locking [Hirose et al., 1999], and even evolution from seismogenic to aseismic creep within the same fault zone [Walcott, 1978; Arnadóttir et al., 1999; Owen et al., 2000]. As aseismic transients are most likely to occur along strong gradients in creep rate [Lapusta et al., 2000], at metastable regions these transients might conceivably trigger seismogenic rupture. In time, continuous monitoring may demonstrate that the simple model of sustained interseismic strain accumulation punctuated by sudden

coseismic release is not just overly simplistic but, in fact, is rarely applicable to megathrust earthquakes.

[23] **Acknowledgments.** We thank Osvaldo Sanchez of the Autonomous University of Mexico (UNAM) for supplying the tide gauge data. Discussion with Jeanne Hardebeck on Coulomb stress transfer was very helpful. Figures were generated with Generic Mapping Tools [Wessel and Smith, 1991]. Jalisco field work was supported under NSF grant EAR-9527810 to J. Stock, while data analysis of subsequent earthquakes was supported under NSF grant EAR-9973191 to T. Melbourne.

References

- Árnadóttir, T., S. Thormley, F. Pollitz, and D. Darby, Spatial and temporal strain rate variations at the northern Hikurangi margin, New Zealand, *J. Geophys. Res.*, **104**, 4931–4944, 1999.
- Aruajo, M., and G. Suarez, Geometry and state of stress of the subducted Nazca plate beneath central Chile and Argentina: Evidence from telseismic data, *Geophys. J. Int.*, **116**, 283–303, 1994.
- Barrientos, S., G. Plafker, and E. Lorca, Postseismic coastal uplift in southern Chile, *Geophys. Res. Lett.*, **19**, 701–704, 1992.
- Blewitt, G., M. Heflin, K. Hurst, D. Jefferson, F. Webb, and J. Zumberge, Absolute far-field displacements from the 28 June 1992 Landers earthquake sequence, *Nature*, **361**, 340–342, 1993.
- Bucknam, R., G. Plafker, and R. Sharp, Fault movement (afterslip) following the Guatemala earthquake of February 4, 1976, *Geology*, **6**, 170–173, 1978.
- Bürgmann, R., P. Segall, M. Lisowski, and J. Svarc, Postseismic strain following the 1989 Loma Prieta earthquake from repeated GPS and leveling measurements, *J. Geophys. Res.*, **102**, 4933–4955, 1997.
- Bürgmann, R., M. Kogan, V. Levin, C. Scholz, R. King, and G. Steblov, Rapid aseismic moment release following the 5 December, 1997 Kronotsky, Kamchatka earthquake, *Geophys. Res. Lett.*, **28**, 1331–1334, 2001.
- Byrne, D., D. Davis, and L. Sykes, Loci and maximum size of thrust earthquakes and the mechanics of the shallow region of subduction zones, *Tectonics*, **7**, 833–857, 1988.
- Carlo, D., T. Lay, C. Ammon, and J. Zhang, Rupture process of the 1995 Antofagasta subduction earthquake ($M_w = 8.1$), *Pure Appl. Geophys.*, **154**, 677–709, 1999.
- Cohen, S., On the rapid postseismic uplift along Turnagain Arm, Alaska following the 1964 Prince William Sound earthquake, *Geophys. Res. Lett.*, **25**, 1213–1215, 1998.
- Comte, D., and G. Suarez, Stress distribution and geometry of the subducting Nazca plate in northern Chile using teleseismically recorded earthquakes, *Geophys. J. Int.*, **122**, 419–440, 1995.
- Comte, D., M. Pardo, L. Dorbath, C. Dorbath, H. Haessler, L. Rivera, A. Cisternas, and L. Ponce, Determination of seismogenic interplate contact zone and crustal seismicity around Antofagasta, northern Chile using local data, *Geophys. J. Int.*, **116**, 553–561, 1994.
- Courboux, F., S. K. Singh, and J. Pacheco, The 1995 Colima-Jalisco, Mexico, earthquake ($M_w = 8$): A study of the rupture process, *Geophys. Res. Lett.*, **24**, 1019–1022, 1997.
- Delouis, B., et al., The $M_w = 8.0$ Antofagasta (northern Chile) earthquake of 30 July 1995: A precursor to the end of the large 1877 gap, *Bull. Seismol. Soc. Am.*, **87**, 427–445, 1997.
- DeMets, C., I. Carmichael, T. Melbourne, O. Sanchez, J. Stock, G. Suarez, and K. Hudnut, Anticipating the successor to Mexico's largest historical earthquake, *Eos Trans AGU*, **76**(42), 417, 424, 1995.
- Dieterich, J., Earthquake nucleation on faults with rate-dependent and state-dependent strength, *Tectonophysics*, **211**, 115–134, 1992.
- Dragert, H., K. Wang, and T. James, A silent slip event on the deeper Cascadia subduction interface, *Science*, **292**, 1525–1528, 2001.
- Dziewonski, A., G. Ekström, and M. Salganik, Centroid-moment tensor solutions for October–December, 1995, *Phys. Earth Planet. Inter.*, **101**, 1–12, 1997.
- Escobedo, D., J. F. Pacheco, and G. Suárez, Teleseismic body-wave analysis of the 9 October, 1995 ($M_w = 8.0$), Colima-Jalisco, Mexico earthquake, and its largest foreshock and aftershock, *Geophys. Res. Lett.*, **25**, 547–550, 1998.
- Freymueller, J., and J. Beavan, Absence of strain accumulation in the western Shumagin segment of the Alaska subduction zone, *Geophys. Res. Lett.*, **26**, 3233–3236, 1999.
- Freymueller, J., C. Zweck, H. Fletcher, S. Areinsdottier, S. C. Cohen, and M. Wyss, The Great Alaska “earthquake” of 1998–2001, *Eos Trans. AGU*, **82**(47), Fall Meet. Suppl., Abstract G22D-11, 2001.
- Harris, R., Stress triggers, stress shadows, and implications for seismic hazard, *J. Geophys. Res.*, **103**, 24,347–24,358, 1998.
- Heaton, T., Evidence for and implications of self-healing pulses of slip in earthquake rupture, *Phys. Earth Planet. Inter.*, **64**, 1–20, 1991.

- Heki, K., and Y. Tamura, Short-term afterslip in the 1994 Sanriku-Haruka-Oki earthquake, *Geophys. Res. Lett.*, *24*, 3285–3288, 1997.
- Heki, K., S. Miyazaki, and H. Tsuji, Silent fault slip following an interplate thrust earthquake at the Japan Trench, *Nature*, *386*, 595–598, 1997.
- Hirose, H., K. Hirahara, F. Kimata, N. Fujii, and S. Miyazaki, A slow thrust slip event following the two 1996 Hyuganda earthquakes beneath the Bungo Channel, southwest Japan, *Geophys. Res. Lett.*, *26*, 3237–3240, 1999.
- Husen, S., E. Kissling, E. Flueh, and G. Asch, Accurate hypocentre determination in the seismogenic zone of the subduction Nazca plate in northern Chile using a combined on-/offshore network, *Geophys. J. Int.*, *138*, 687–701, 1999.
- Hutton, W., C. DeMets, O. Sánchez, G. Suárez, and J. Stock, Slip kinematics and dynamics during and after the 9 October 1995 $M_w = 8.0$ Colima-Jalisco earthquake, Mexico, from GPS geodetic constraints, *Geophys. J. Int.*, *146*, 637–658, 2002.
- Hyndman, R., and K. Wang, The rupture zone of Cascadia great earthquakes from current deformation and the thermal regime, *J. Geophys. Res.*, *100*, 22,133–22,154, 1995.
- Ihmlé, P., and J. Ruegg, Source tomography by simulated annealing using broad-band surface waves and geodetic data: Application to the $M_w = 8.1$ Chile 1995 event, *Geophys. J. Int.*, *131*, 146–158, 1997.
- James, T., J. Clague, K. Wang, and I. Hutchinson, Postglacial rebound at the northern Cascadia subduction zone, *Quat. Sci. Rev.*, *19*, 1527–1541, 2000.
- Kanamori, H., *Seismic and aseismic slip along subduction zones and their tectonic implications*, in *Island Arcs and Deep Sea Trenches and Back-Arc Basins*, Maurice Ewing Ser., vol. 1, edited by M. Talwani and W. C. Pitman III, pp. 163–174, AGU, Washington, D. C., 1977.
- Kanamori, H., and L. Astiz, The 1983 Akita-Oki earthquake ($M_w = 7.8$) and its implications for systematics of subduction earthquakes, *Earthquake Predict. Res.*, *3*, 305–317, 1985.
- Kawasaki, I., Y. Asai, Y. Tamura, T. Sagiya, N. Mikami, Y. Okada, M. Sakata, and M. Kasahara, The 1992 Sanriku-Oki, Japan, ultra-slow earthquake, *J. Phys. Earth*, *43*, 105–116, 1995.
- Klotz, A., J. Reinking, and D. Angermann, Die Vermessung der Deformation der Erdoberfläche, *Geowissenschaften*, *14*, 384–389, 1996.
- Klotz, J., et al., GPS-derived deformation of the central Andes including the 1995 Antofagasta $M_w = 8.0$ earthquake, *Pure Appl. Geophys.*, *154*, 709–730, 1999.
- Kogan, M., R. Bürgmann, R. W. King, C. Scholz, and V. E. Levin, *Eos Trans. AGU*, *80*(46), Fall Meet. Suppl., F275, 1999.
- Lapusta, N., J. Rice, Y. Ben-Zion, and G. Zheng, Elastodynamic analysis for slow tectonic loading with spontaneous rupture episodes on faults with rate- and state-dependent friction, *J. Geophys. Res.*, *105*, 23,765–23,789, 2000.
- Lichten, D., and J. S. Border, Strategies for high precision Global Positioning System orbit determination, *J. Geophys. Res.*, *92*, 12,751–12,762, 1987.
- Linde, A. T., and P. G. Silver, Elevation changes and the great 1960 Chilean earthquake: Support for aseismic slip, *Geophys. Res. Lett.*, *16*, 1305–1308, 1989.
- Lowry, A., K. Larson, V. Kostoglodov, and R. Bilham, Transient fault slip in Guerrero, southern Mexico, *Geophys. Res. Lett.*, *28*, 3753–3756, 2001.
- Marone, C., and C. H. Scholz, The depth of seismic faulting and the upper transition from stable to unstable slip regimes, *Geophys. Res. Lett.*, *15*, 621–624, 1988.
- Marone, C., C. Scholz, and R. Bilham, On the mechanics of afterslip, *J. Geophys. Res.*, *96*, 8441–8452, 1991.
- Masterlark, T., C. DeMets, H. Wang, O. Sanchez, and J. Stock, Homogeneous vs heterogeneous subduction zone models: Coseismic and post-seismic deformation, *Geophys. Res. Lett.*, *28*, 4047–4050, 2001.
- Mazzotti, S., X. L. Pichon, P. Henry, and S. Miyazaki, Full interseismic locking of the Nankai and Japan-west Kurile subduction zones: An analysis of uniform elastic strain accumulation in Japan constrained by permanent GPS, *J. Geophys. Res.*, *105*, 13,159–13,177, 2000.
- Melbourne, T., I. Carmichael, C. DeMets, K. Hudnut, O. Sanchez, J. Stock, G. Suarez, and F. Webb, The geodetic signature of the $M_w = 8.0$ Oct. 9, 1995 Jalisco subduction earthquake, *Geophys. Res. Lett.*, *24*, 715–718, 1997.
- Mendoza, C., and S. Hartzell, Fault-slip distribution of the 1995 Colima-Jalisco, Mexico, earthquake, *Bull. Seismol. Soc. Am.*, *89*, 1338–1344, 1999.
- Nakano, T., and K. Hirahara, GPS observations of postseismic deformation for the 1995 Hyogo-ken Nanbu earthquake, Japan, *Geophys. Res. Lett.*, *24*, 503–506, 1997.
- Nishimura, T., H. Nakahara, H. Sato, and M. Ohtake, Source process of the 1994 Sanriku earthquake, Japan, as inferred from a broad-band seismogram, *Tohoku Geophys. J.*, *34*, 121, 134, 1996.
- Okada, Y., Internal deformation due to shear and tensile faults in a half-space, *Bull. Seismol. Soc. Am.*, *82*, 1018–1040, 1993.
- Oleskevich, D., R. Hyndman, and K. Wang, The upslip and downslip limits to great subduction earthquakes: Thermal structure models of Cascadia, south Alaska, SW Japan, and Chile, *J. Geophys. Res.*, *104*, 14,965–14,991, 1999.
- Ortiz, M., V. Kostoglodov, S. K. Singh, and J. Pacheco, New constraints on the uplift of the October 9, 1995 Jalisco-Colima earthquake ($M_w = 8$) based on the analysis of tsunami records at Manzanillo and Navidad, Mexico, *Geofis. Int.*, *39*, 349–357, 2000.
- Owen, S., P. Segall, M. Lisowski, A. Miklius, M. Murray, M. Bevis, and J. Foster, January 30, 1997 eruptive event on Kilauea Volcano, Hawaii, as monitored by continuous GPS, *Geophys. Res. Lett.*, *27*, 2757–2760, 2000.
- Pacheco, J. F., L. R. Sykes, and C. H. Scholz, Nature of seismic coupling along simple plate boundaries of the subduction type, *J. Geophys. Res.*, *98*, 14,133–14,159, 1993.
- Prescott, W., N. King, and G. Guohua, Preseismic, coseismic, and post-seismic deformation associated with the 1984 Morgan Hill, Calif. earthquake, *Spec. Publ. Calif. Div. Mines Geol.*, *68*, 137–148, 1984.
- Prescott, W. H., and M. Lisowski, Deformation at Middleton Island, Alaska, during the decade after the Alaska earthquake of 1964, *Bull. Seismol. Soc. Am.*, *67*, 579–586, 1977.
- Pritchard, M., M. Simons, P. Rosen, S. Hensley, and F. Webb, Co-seismic slip from the July 30, 1995, $M_w = 8.1$ Antofagasta, Chile earthquake as constrained by InSAR and GPS observations, *Geophys. J. Int.*, in press, 2002.
- Reigber, C., Y. Xia, G. Michel, J. Klotz, and D. Angermann, The Antofagasta 1995 earthquake: Crustal deformation pattern as observed by GPS and D-Insar, paper presented at 3rd ERS Symposium on Space at the service of our Environment, Eur. Space Agency, Florence, Italy, 1997.
- Savage, J., and M. Lisowski, Strain accumulation in the Shumagin seismic gap, Alaska, *J. Geophys. Res.*, *91*, 7447–7454, 1986.
- Savage, J., and G. Plafker, Tide gage measurements of uplift along the south coast of Alaska, *J. Geophys. Res.*, *96*, 4325–4335, 1991.
- Scholz, C., Mechanics of faulting, *Annu. Rev. Earth Planet. Sci. Lett.*, *17*, 309–334, 1989.
- Scholz, C., Earthquakes and friction laws, *Nature*, *391*, 37–42, 1998.
- Shen, Z., D. Jackson, Y. Feng, M. Cline, M. Kim, P. Fang, and Y. Bock, Postseismic deformation following the Landers earthquake, California, 28 June 1992, *Bull. Seismol. Soc. Am.*, *84*, 780–791, 1994.
- Smith, S., and M. Wyss, Displacement on the San Andreas fault subsequent to the 1966 Parkfield earthquake, *Bull. Seismol. Soc. Am.*, *58*, 1955–1973, 1968.
- Sobiesiak, M., Fault plane structure of the Antofagasta, Chile earthquake of 1995, *Geophys. Res. Lett.*, *27*, 577–580, 2000.
- Stein, R., G. P. King, and J. Lin, Stress triggering of the 1994 $M = 6.7$ Northridge, California earthquake by its predecessors, *Science*, *265*, 1432–1435, 1994.
- Tanioka, Y., L. Ruff, and K. Satake, The Sanriku-Oki, Japan, earthquake of December 28, 1994 ($M_w = 7.7$)—Rupture of a different asperity from a previous earthquake, *Geophys. Res. Lett.*, *23*, 1465–1468, 1996.
- Thatcher, W., The earthquake deformation cycle at the Nankai trough, southwest Japan, *J. Geophys. Res.*, *89*, 3087–3101, 1984.
- Thatcher, W., and N. Fujita, Deformation of the Mitaka Rhombus: Strain buildup following the 1923 Kanto earthquake, central Honshu, Japan, *J. Geophys. Res.*, *89*, 3102–3106, 1984.
- Tichelaar, B., and L. Ruff, Depth of seismic coupling along subduction zones, *J. Geophys. Res.*, *98*, 2017–2037, 1993.
- Tse, S., and J. Rice, Crustal earthquake instability in relation to the depth variation of frictional slip properties, *J. Geophys. Res.*, *91*, 9452–9472, 1986.
- Ueda, H., M. Ohtake, and H. Sato, Afterslip on the plate interface following the 1978 Miyagi-Oki, Japan, earthquake, as revealed from geodetic measurement data, *Tectonophysics*, *338*, 45–57, 2001.
- Walcott, R., Geodetic strains and large earthquakes in the axial tectonic belt of North Island, New Zealand, *J. Geophys. Res.*, *83*, 4419–4429, 1978.
- Wessel, P., and W. Smith, Free software helps map and display data, *Eos Trans. AGU*, *72*, 441, 445–446, 1991.
- Winder, R., and S. Peacock, Viscous forces acting on subducting lithosphere, *J. Geophys. Res.*, *106*, 21,937–21,951, 2001.
- Zumberge, J., R. Liu, and R. E. Neilan (Eds.), *International GPS Service for Geodynamics 1994 Annual Report*, 329 pp., Jet Propul. Lab., Pasadena, Calif., Sept. 1995.

T. I. Melbourne, Department of Geological Sciences, Central Washington University, Ellensburg, WA 98926, USA. (tim@geology.cwu.edu)

C. Reigber, GeoForschungsZentrum Potsdam, Telengrafenberg, D-14473, Potsdam, Germany.

J. M. Stock, Seismological Laboratory 252-21, California Institute of Technology, Pasadena, CA 91125, USA. (jstock@gps.caltech.edu)

F. H. Webb, Jet Propulsion Laboratory, 4800 Oak Grove Dr., Pasadena, CA 91109, USA.